

Wings at yaw

Aerodynamic performance alters when a racecar isn't running straight ahead. But what happens to the performance of wings when at yaw angles?

We have seen in some of our wind tunnel-based Aerobytes studies how aerodynamic forces and balance can alter on a racecar with yaw angles up to around 20 degrees in some instances. Aero balance can sometimes tangibly change over even quite small yaw angle shifts. But it is rarely possible to tell for certain in the wind tunnel why these changes occur, or how the forces on individual components alter. So could we use some simple CFD simulations to provide some insight?

BY SIMON MCBEATH

The question was catalysed by an enquiry from a category of motorsport where the objective is to maintain an extreme oversteer condition in a controlled and stylish manner, that is, 'Drifting'. But having raised that question, it seemed that looking at what happens over a wide range of yaw angles might be instructive in other on- and off-road motorsport applications.

So, a set of simple models was constructed in CAD, starting with a dual-element wing. Then a basic

model of a saloon/sedan was created that utilised the dual-element wing. And finally a single-seat model with dual-element front and rear wings was examined. The plan was to see initially how the performance of an isolated wing in freestream air altered over a wide range of yaw angles, and then to look at the performance of wings on two different types of cars while also taking the opportunity to examine how the aerodynamics of the car models themselves altered with yaw angle.

The range of yaw angles used for the initial evaluations here

may seem extreme. But angles of 45 degrees and more can be successfully maintained with control and 'pseudo-stability' by experienced exponents in suitably setup cars.

ISOLATED WING

The high downforce dual element wing was initially fitted with a simple, fairly deep rectangular end plate design - see CAD 1. This end plate depth had been shown to offer a good compromise between a useful aerodynamic benefit (at least, in a straight line) versus the inevitable extra weight

and potential loss of rigidity. But being relatively large, what would its effect be when the wing was at yaw? Figure 1 plots downforce, drag and side force at 100mph (44.7m/s) across the yaw range up to 45 degrees.

The change to downforce saw an initial gentle decline to 15 degrees yaw, after which the decline became steeper though essentially still linear, ending up at about 38 per cent of its 'straight ahead' value. Drag initially rose gently but then somewhat more steeply, and at 60 degrees had risen by about 23 per cent from its zero yaw value. The side force was relatively modest at all angles compared to the forces on the other two axes, peaking at 30 degrees yaw on a curve that initially rose, then dipped slightly.

Before attempting to comment on this slightly irregular side force pattern, we'll first examine other wing configurations, to follow shortly. But the general shape of the downforce and drag plots here do not seem unreasonable, and the changing rate of decline in downforce seemed to tally with

the visualisations, which show that flow separation around the end plates only really took hold once the wing was at an appreciable yaw angle (see Figures 2 and 3). And at the point when separation did become marked, it was clear that parts of the wing were then in the wake of the 'upwind' end plate. And as both end plates create these wakes, it's not hard to see why drag increased.

So if the end plates were at least in part responsible for the

range of yaw angles in successive CFD runs in otherwise identical conditions. The data are shown in Figure 4, the plot lines with the 'EPmin' suffix being those of the wing with minimalist end plates, here plotted alongside the 'datum' wing for easy comparison.

Some quite different patterns were in evidence here. First, straight line (zero yaw) downforce was almost 15 per cent down compared to the wing with the datum end plates, which was

datum end plates maintained greater downforce up to around 20 degrees even though the rate of decline with yaw angle was steeper than with the minimalist end plates. And fourth, side force - though small in magnitude at yaw - was actually in the opposite direction with the minimalist end plates, this presumably arising from a small sideways vector component from the wing's suction surface that became evident in the (effective) absence of end plates.

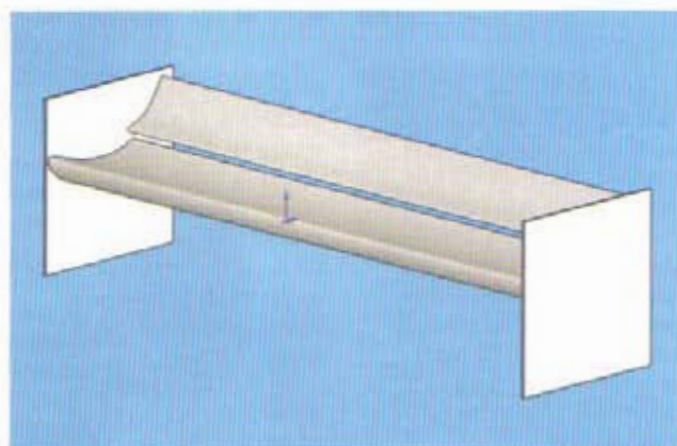
Already then, there could be a choice to be made here between end plates that maintained the maximum downforce at lower yaw angles, but which then saw downforce decline quite sharply once beyond 15 degrees yaw vs ones that offered a more gradual and benign response to changes in yaw angle but at an initially lower downforce level.

A device that has been seen on wings down the years is the intermediate 'fence' or 'spill plate'. Perhaps one of the best known manifestations was on WRCars, and the natural conclusion from

With experience, angles of over 45 degrees can be maintained with control and 'pseudo-stability'

decline in downforce as yaw angle was increased, how would the wing behave with much smaller end plates? A minimalist end plate design that protruded only very slightly below the wing's suction (lower) surface, and which had less area above the pressure surface too was drawn up - see CAD 2 - and the wing was put through the same

what we would expect. Second, the decline in downforce with yaw angle was less across the full yaw range with the minimalist end plates, so that at the steeper yaw angles tested, downforce was actually higher than with the datum end plates, almost 18 per cent higher at 45 degrees and over 8 per cent higher at 30 degrees. Third, the



CAD 1: the dual-element wing with large end plates

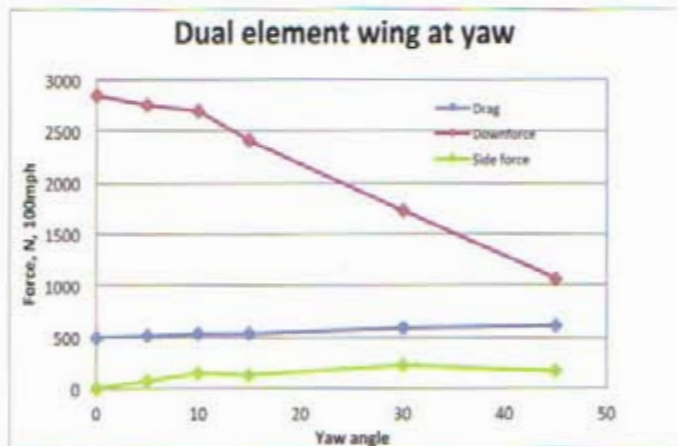


Figure 1: aerodynamic data for the 'datum' dual element wing

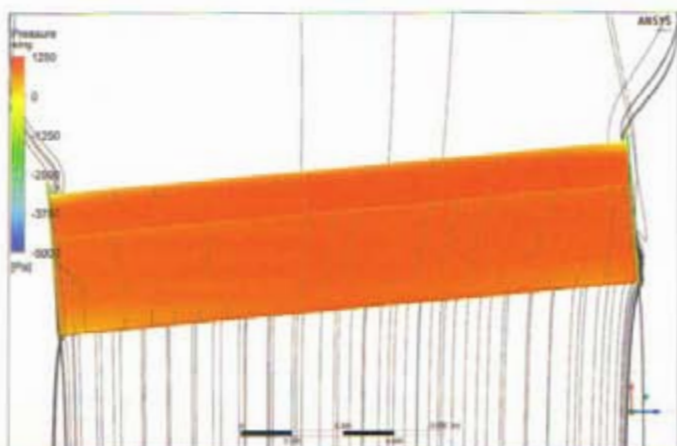


Figure 2: top view of the wing at 5 degrees yaw, flow entering from the bottom of the image; the streamlines are attached to the end plates

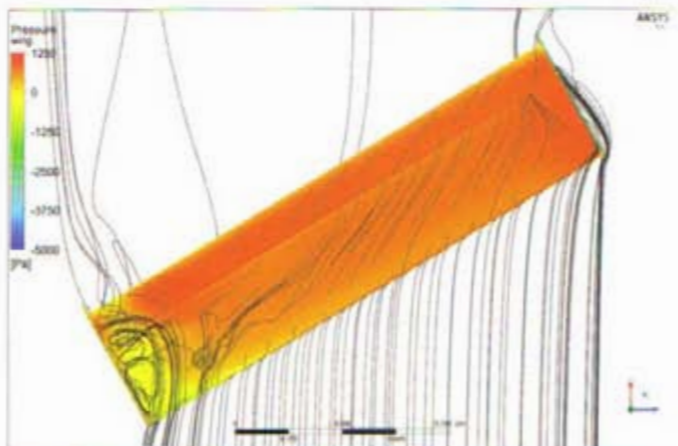
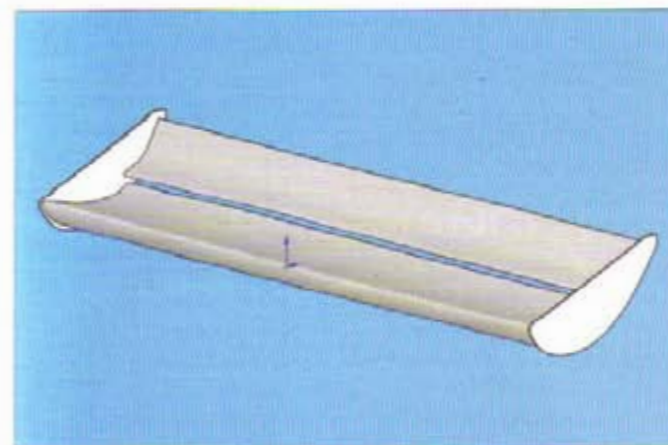


Figure 3: top view of the wing at 30 degrees yaw - note how the end plates have disrupted the aerodynamic flow



CAD 2: dual-element wing with minimalist end plates

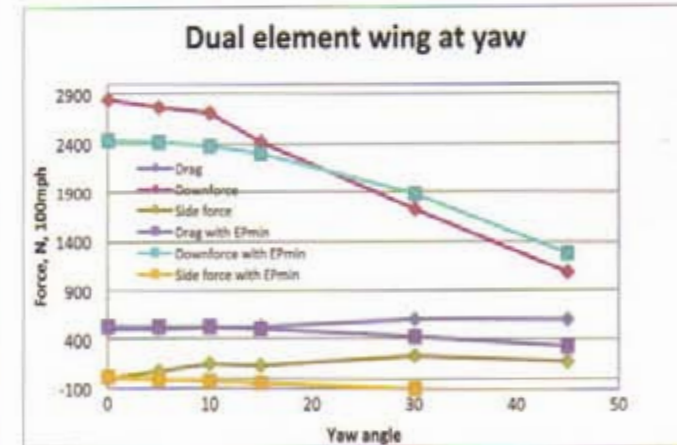
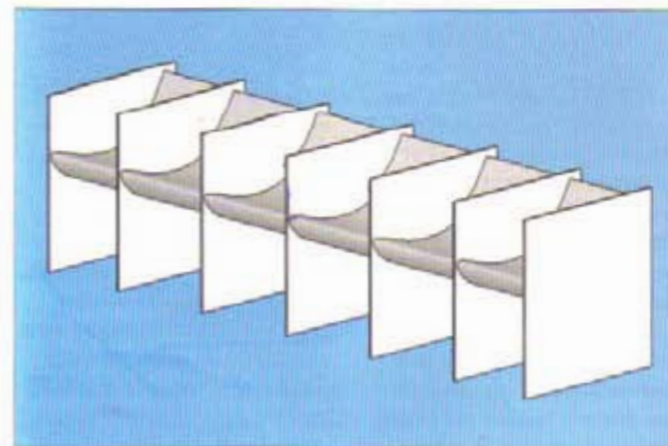


Figure 4: aero data for the wing with 'minimalist' end plates vs the datum wing



CAD 3: dual-element wing with intermediate spill plates

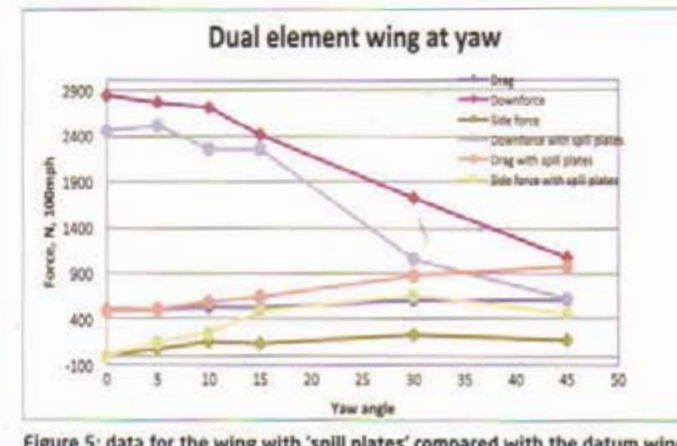


Figure 5: data for the wing with 'spill plates' compared with the datum wing

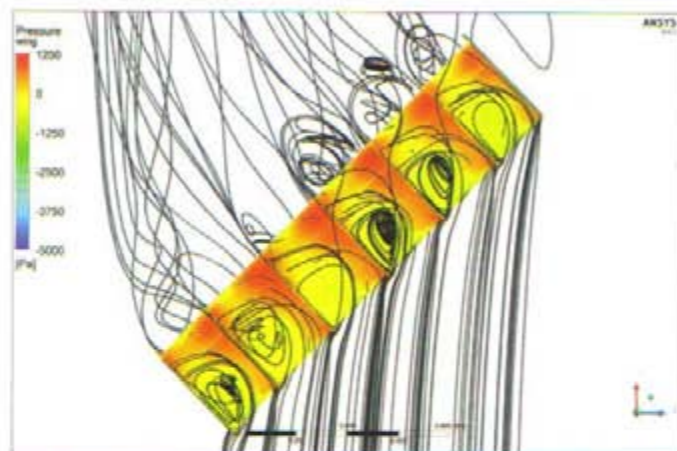


Figure 6: top view of the wing with spill plates at 45 degrees yaw, flow entering from the bottom

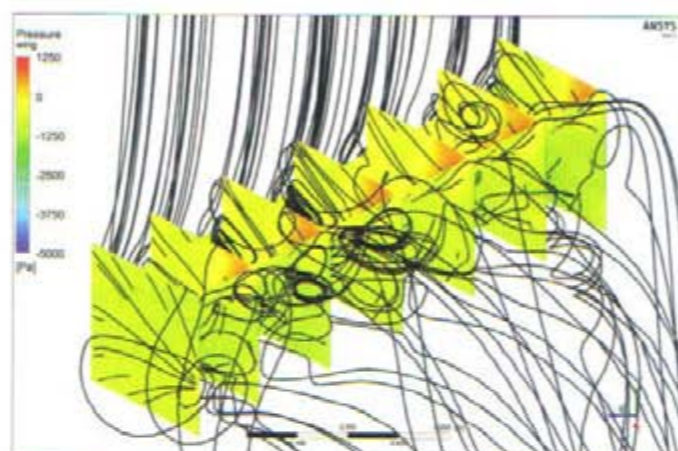


Figure 7: rear isometric view of the wing with spill plates at 45 degrees yaw, flow entering from top



CAD 4: the sedan with wing model

that application was that their role was yaw-related. Published suggestions for their purpose ranged from 'flow straighteners' to aid the wing's performance, to devices to increase the yaw-returning moment to help stabilise or to react against the oversteer condition. Another CAD model featuring five additional plates to the same dimensions as the end plates and set at regular span-wise spacings across the dual element wing was constructed - CAD 3 - and then evaluated in CFD across the same yaw range as the previous models. The data is shown in Figure 5 and plotted alongside the datum wing's data.

Once again, straight line (zero yaw) downforce was down compared to the datum wing, and the CFD visualisations showed that the intermediate fences created their own wakes that locally reduced the magnitude of the suction on the wing's lower surface. Then, as yaw was applied, the response with the spill plates was more irregular, but not totally dissimilar to the datum wing's

response. Drag started off much the same but increased more rapidly over 10 degrees yaw, ultimately peaking at a higher magnitude than downforce at the highest yaw angle. And side force initially responded similarly to the datum wing, but then jumped to a much higher level at 15 degrees yaw and above. If one was to add the drag and side force components together to resolve the net force along the wing's span-wise axis, it would be quite significant at high yaw. See Figures 6 and 7.

However, these toe-in-the-water studies of a wing in isolation do not represent what happens to a wing mounted on a car. For that we need to bring in our 'racecar plus wing' models.

WING ON A SEDAN

A model of a generic sedan (CAD 4) was created, featuring a front aero kit comprising an airdam and a large splitter with end-fences and dive planes, on which the high downforce dual element wing seen in the previous section could then be attached. The wing was adjusted to a lower overall angle

PREDICTING FUTURE DEVELOPMENTS

The future of F1 aero development lies with fully integrated testing development environments, with 'turn key' solutions and support - including driver-in-the-loop with hardware-in-the-loop for optimisation of the vehicle.

Efficient, correlated testing (virtual CFD/DIL to wind tunnel to track) are the main drivers which may be cost and legislation driven. I think there will be an aggressive push for enhanced efficient wind tunnel testing methodologies - things like next generation continuous motion systems, high-speed data acquisition

with ultra-quick model changes and tyre shape matching.

Other areas that will grow will be shape, aeroelasticity and turbulence intensity matching of 60 per cent scale to full-scale: true cornering studies with proper interference correction methodologies (WT flap system); Flow visualisation and automatic minimal interference full flow field interrogation.

Finally I think there will be a need to closely follow regulations and development trends, such as like the likely return of full-scale tyre testing.

Professor Mark Gillan,
principal R&D engineer, MTS

to improve aerodynamic balance. The model also featured simplistic representations of the internals of a front engine compartment to incorporate some internal flows.

To simplify the CFD setup process when at yaw, the wheels were stationary throughout, although the ground was set to move at the same speed and in the same direction as the inlet airflow in our virtual wind tunnel. The car was run first at zero yaw and then the yaw angle was increased in 5 degree increments. We'll look at the results of different aspects in turn, starting with downforce. As Table 1 indicates, the forces on the main components have been calculated separately.

A number of interesting points spring from Table 1. Total downforce initially increased with yaw, primarily because of a modest increase in rear wing downforce, but it then declined increasingly

rapidly and by 20 degrees had become positive lift overall. This was mainly because the car itself generated increasing amounts of positive lift once above 10 degrees yaw (see Figure 8). However, the wing itself also generated less downforce once above 5 degrees yaw, with quite a marked drop once over 15 degrees yaw, which matched the pattern in the isolated wing tests. Frustrating meshing issues, unresolved at copy deadline time, precluded higher yaw angles being investigated for now (on this model).

Moving on to drag, the results are shown in Table 2. In essence then, drag increased with yaw angle and the rate of drag increase went up as yaw angle increased, the dominant source of drag being the car body (including wheels etc) - but wing drag also became more significant at higher yaw.

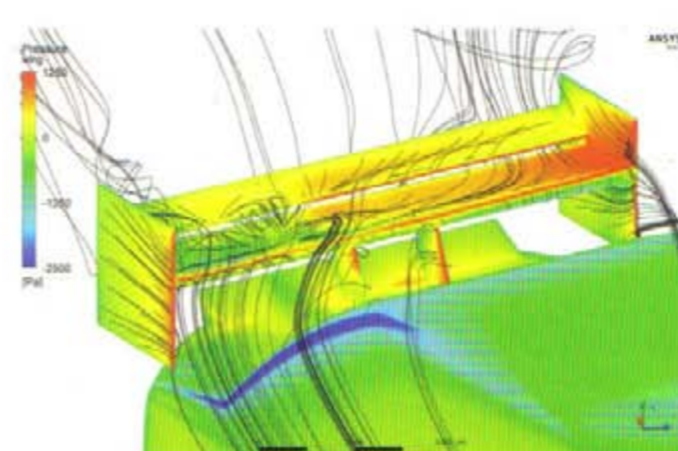


Figure 8: the rear wing on the sedan showed asymmetric pressure distributions and disruption of streamlines at 20 yaw. Notice the low pressures on the roof and the very low pressure on the rear screen pillar - sources of body lift

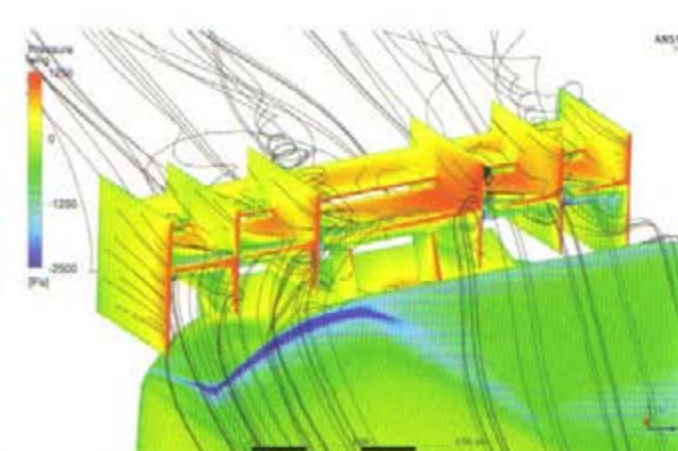


Figure 9: adding spill plates generated greater side force and yaw moment

Table 1: downforce, N at 100mph, vs yaw on the sedan plus wing model (negative downforce = positive lift here)

Yaw angle	Df, car	Df, splitter	Df, wing	Total Df
0	-788.3	1352.5	1193.8	1758.0
5	-791.2	1358.5	1239.6	1806.9
10	-739.0	1360.0	1093.0	1714.0
15	-1436.3	1291.2	973.9	828.8
20	-2593.2	1093.4	732.1	-767.7

Table 2: drag forces, N at 100mph, vs yaw on the sedan plus wing model

Yaw angle	Drag, car	Drag, splitter	Drag, wing	Total drag
0	1296.7	13.1	93.1	1402.9
5	1355.3	16.9	123.2	1495.4
10	1482.0	26.0	181.5	1689.5
15	1646.1	36.0	226.1	1908.2
20	1852.0	46.7	305.5	2204.2

Table 3: side forces, N, and yaw moments, Nm, at 100mph, on the sedan plus wing model

Yaw angle	Side, car	Side, splitter	Side, wing	Total side, N
0	-23.1	0.1	0.4	-22.6
5	333.4	35.6	116.0	485.0
10	617.7	69.0	287.9	974.6
15	1132.5	83.9	418.9	1635.3
20	1577.4	90.1	520.0	2187.5

Yaw angle	Yaw, car	Yaw, splitter	Yaw, wing	Total yaw, Nm
0	123.3	87.3	-18.1	192.5
5	-309.1	24.8	-425.1	-709.4
10	-432.1	47.8	-1053.8	-1438.1
15	-1004.5	59.8	-1548.9	-2493.6
20	-1488.6	66.2	-1989.8	-3412.2

Table 4: the balance of downforce with yaw angle

Yaw angle	Total Df, N	Total pitch, Nm	CoFp, m	%front
0	1758.0	1758.0	2.039	24.2%
5	1806.9	1811.9	2.191	18.5%
10	1714.0	1724.0	2.222	17.4%
15	828.8	843.8	2.608	3.1%
20	-767.7	-747.7	0.368	86.3% (positive lift)

Table 3 shows the side forces and the yaw moments combined.

Once again the side forces and yaw moments showed overall increases with increasing yaw angle, both becoming quite substantial at 20 degrees. One of the interesting things in our context here is that as the wing's side force increased, obviously so too did its yaw moment. The forces and moments are calculated by the CFD at the coordinate origin of the CAD model, which in this instance is in line with the front wheel contact point and at ground level. By dividing the yaw moment by the side force at each yaw angle, it became evident that the centre of pressure of the side force moved backwards with increasing yaw angle - this the result of the increasing influence of the rear wing (and end plates).

It is also interesting to examine how the front-to-rear downforce distribution shifted with yaw. This can be done by dividing the pitch moment by the vertical force, which gives a distance in metres of the centre of pressure from the CAD origin (which, having been set at ground level means there is no pitch moment from the drag force to complicate the calculation). The distance of the centre of pressure along the wheelbase is then used to obtain the proportion of downforce exerted at the front as a measure of the aerodynamic balance. Table 4 illustrates.

Looking at the right-hand column of Table 4, we can see that the aerodynamic balance shifted rearwards (%front reduced) as yaw angle increased, albeit non-linearly, but at 15 degrees nearly all the

downforce was being felt at the rear. So, as well as the yaw moment centre shifting rearwards as yaw angle increased, the balance of downforce also shifted rearwards. Both of these factors would oppose the dynamic forces that generated the yaw angle in the first place, and both were related to the presence of the wing at the back of the car. Of course, we should remind ourselves that these simulations used a simplistic generic model and not a real car, but the changes we have seen here are ones that would bear investigation on a real car or a digital model that adequately represented it, in applications where large yaw angles would be routinely encountered.

It was mentioned earlier that intermediate spill plates have been said to improve a wing's performance on a car. In isolation they did not help downforce but they did increase side forces when at yaw. Two further runs were carried out - one with the wing with spill plates on the car at zero yaw, and one at 20 degrees yaw. The overall results compared to the 'no spill plates' cases are shown in Table 5 (overleaf).

We can see that the sole benefit of the spill plates was to generate more substantial side force and yaw moment, with a further aft centre of pressure of that side force (obtained from the yaw moment divided by the side force). The wing's downforce contribution did reduce slightly. However, this was just one look at one spill plate configuration and one yaw angle, and more study would be warranted to see if the concept merited use in a specific application - see Figure 9.

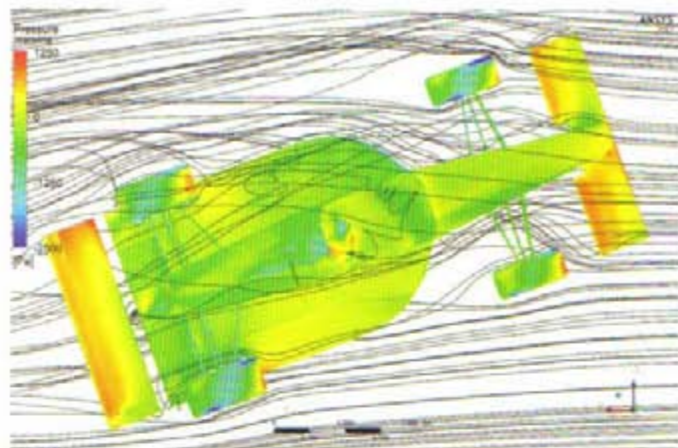


Figure 10: top view of the single-seater at 20 degrees yaw, streamlines emanating at front wing height (from the right)

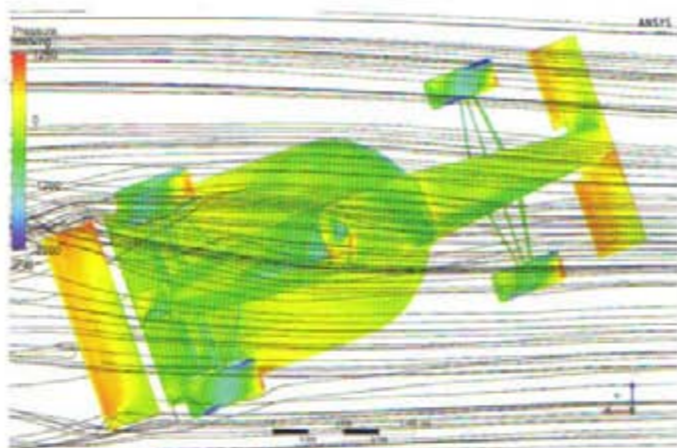


Figure 11: top view of the single-seater at 20 degrees yaw, streamlines emanating at rear wing height

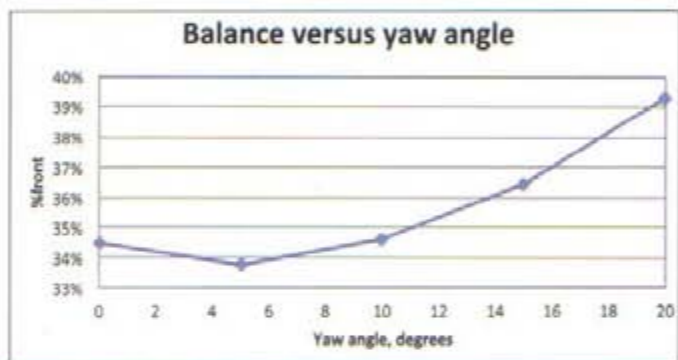


Figure 12: aerodynamic balance versus yaw for the single-seater model



CAD 5: the single-seater model with dual-element front and rear wings

Yaw angle		Total drag	Total Df	Total side	Total pitch	Total yaw
20	No spill plates	2204.2	-767.7	2187.5	-282.6	-3412.2
20	Spill plates	2420.9	-806.8	2646.8	-95.3	-4924.1

Yaw angle	Df, car	Df, f/wheels	Df, f/wing	Df, r/wheels	Df, r/wing	Total Df
0	521.7	-91.4	1057.3	-112.8	1281.6	2656.4
5	371.4	-97.8	1027.7	-129.8	1252.0	2423.5
10	405.8	-104.1	984.0	-131.9	1157.1	2310.9
15	553.5	-106.9	928.4	-152.4	1082.6	2305.2
20	554.3	-113.3	866.1	-127.8	870.4	2049.7

WINGS ON A SINGLE-SEATER

The CAD model for this part of the investigation was that of the writer's hillclimb single-seater project, as used in our study of 'front wing fundamentals' last month - see CAD 5. The wing setups, which featured a less cambered rear wing than on the sedan, were again chosen to create a reasonable aerodynamic balance at zero yaw. Very similar CFD conditions to those imposed upon the sedan model were used - that is, moving ground but

stationary wheels - and 100mph air speed in the 'flow domain', our virtual wind tunnel. As with the sedan model, the single-seater was rotated through 5 degree yaw increments. The simulations were setup so that the forces and moments could be individually calculated on, in alphabetical order, the central car body, the front wheels, the front wing, the rear wheels and the rear wing. As with the sedan we'll first look at how downforce changed with yaw. Table 6 shows the data.

The first thing that differed from the sedan is that the 'car' - that is, the central chassis, sidepods and underbody unit - created downforce rather than lift. The only items to create lift here were the exposed wheels. Given that they were non-rotating in these simulations their lift contribution would be slightly greater than had they been rotating, but the difference in their overall effect on net downforce was relatively small. Looking at the right-hand column, total downforce reduced

with yaw, initially at a declining rate but then more steeply from 15 degrees. The front wing's contribution declined quite slowly with yaw, whereas rear wing downforce decreased at an accelerating rate - especially after 15 degrees yaw. This mirrored the isolated wing's performance, but not that of the wing on the sedan, which initially gained downforce at 5 degrees yaw. Interestingly, the single-seater's body unit saw its downforce initially decline at 5 degrees yaw, but then increase again before levelling out at 15 degrees at a value slightly higher than the straight ahead value. See Figures 10 and 11.

The effect on overall balance was markedly different to the sedan case, and the plot in Figure 12 best illustrates this. There was an initial reduction in %front at 5 degrees yaw, but then a shift to the front which increased quite markedly as yaw increased. So whereas the sedan's response was to counter the effects that would have caused high yaw angle to occur by increasing the

Yaw angle	Drag, car	Drag, f/wheels	Drag, f/wing	Drag r/wheels	Drag, r/wing	Total drag
0	402.5	120.3	107.5	178.0	160.9	969.2
5	403.9	123.3	105.4	183.9	161.9	978.4
10	431.4	144.4	105.4	181.6	178.7	1041.5
15	492.5	158.6	106.2	186.7	205.0	1149.0
20	573.5	165.3	106.7	214.6	251.1	1311.2

Yaw angle	Side, car	Side, f/wheels	Side, f/wing	Side, r/wheels	Side, r/wing	Total side
0	-0.4	0.6	0.1	13.5	0.1	13.9
5	75.8	63.1	5.2	-7.6	81.1	217.6
10	176.7	94.1	10.8	39.2	113.0	433.8
15	345.8	130.3	15.4	-0.2	141.2	632.5
20	486.3	136.6	18.2	53.4	220.1	914.6

Yaw angle	Yaw, car	Yaw, f/wheels	Yaw, f/wing	Yaw, r/wheels	Yaw, r/wing	Total yaw
0	14.1	-0.3	-0.1	-47.4	-0.4	-34.1
5	-151.4	-60.1	-2.5	-43.7	-357.1	-614.8
10	-351.4	-95.1	-0.6	-238.7	-538.9	-1224.7
15	-785.7	-137.3	-1.0	-161.4	-723.2	-1808.6
20	-1083.0	-141.2	-12.3	-399.5	-1113.4	-2749.4

percentage of rear downforce as yaw angle increased, the single-seater's response was the opposite, and one that would be intrinsically less stable on track.

The changes to total drag followed a similar pattern to the sedan with an accelerating increase with yaw angle, as Table 7 demonstrates. The car and rear wing exhibited similar patterns to the overall picture, but the front wing's modest drag contribution was almost unchanged across the yaw range.

Turning to side force and yaw moments, Table 8 shows the responses. The overall side force increased more or less linearly with yaw angle, while the yaw moment increased linearly up to 15 degrees and then slightly more rapidly to 20 degrees. The centre of pressure of the side force was fairly well back on the car, shifting more rearwards at 20 degrees. So this was a more stable response than the change in downforce balance, and it reflected the increasing effect of the rear wing and end plates as yaw angle increased.

The side force responses of the other components were quite varied: the rear wheels showing a highly variable response, and although the forces involved were small, the yaw moments were significant.

TMG TESTING

During Toyota Motorsport GmbH's F1 participation, aero was the principle focus of development. With less than four per cent performance gap between the front of the Formula 1 grid and the non-point-scoring back of the grid, aerodynamics are critical.

The hi-tech facility in Cologne, Germany, allows for both full-scale wind tunnel testing, and CFD to help simulate wings at yaw. The CFD capability is up to 80 million hexahedral cells per vehicle model, the company has a 600-CPU cluster, and can simulate cornering and overtaking. The CFD results can be correlated with wind tunnel results, as can flow fields with PIV results.

TMG's wind tunnel has a rolling road with a wheelbase range extension long enough for a full-size F1 car. The tunnels feature continuous steel belt MTS rolling road, with under-belt load cells, positioning accurate to 0.05mm and facility to simulate tyre deformation and exhaust simulations.

The firm is also installing a slotted wall to reduce blockage, allowing increased efficiency and flexibility for full-car testing, improving its fixation system to allow for a greater variety of items to be tested, and installed universal bearings on rolling roads to allow quicker and easier changes for different wheelbase vehicles.

SUMMARY

In general then, wings at yaw can be expected to yield reduced downforce, although not in all circumstances if our sedan model at 5 degrees yaw is a guide. End plate size certainly influences what happens at yaw, as does the vehicle the wing is mounted to, in terms of the way the wings themselves respond but also how significant

the wing's contribution is to overall aero performance.

And, as is well-known in sprint car series around the world, the side forces and yaw moments created by a wing with sizable end plates become significant as yaw angle increases.

Racecar Engineering's thanks to ANSYS UK for the use of CFD-Flo software

TYRE ROLE

It is important to understand aerodynamics at yaw because of the way in which tyres work with a road surface in order to generate grip. A rotating tyre operating at zero angle to the oncoming tarmac generates near zero lateral forces for our vehicle.

When driving a car, operating our front and rear tyres at varying amounts of yaw (or slip) angle, it is a matter of how we control the car in order to change its direction. We could call our steering wheel the 'yaw commander' - as we turn the wheel we are in fact yawing the front tyre contact patches relative to the direction of travel.

Most racers do not utilise actively controlled four-wheel steering and as such the rear wheels of most cars have a fixed relationship with the vehicle chassis. In order for our drivers to alter the slip angles of a car's rear tyres, they must first yaw the entire vehicle. If you are generating cornering forces in a fast-moving chassis, then you will be driving in yaw - and during car control recovery situations these angles can be pretty large.

We are unlikely to ever see a situation where these yaw angles are not accompanied by chassis roll angle at the same time, even if the only suspension deflection is the tyre's sidewall.

Approaching vehicle dynamics holistically, we must understand the operational detail of the sub-systems. When making design or setup decisions, we should concentrate on the interdependence of these systems and the net effects our changes will have on the overall vehicle performance.

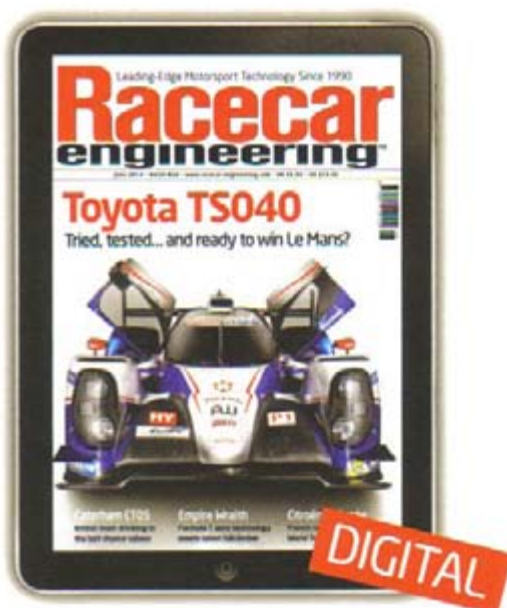
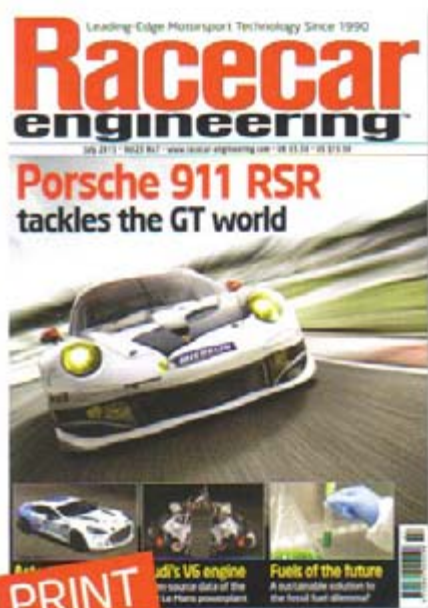
Aerodynamics in yaw is important, because the optimal solutions for maximum negative lift generation in a conventional zero yaw wind tunnel are unlikely to be the optimal solution for the best vehicle system performance.

Sam Borgman, Torque Developments International

Although the side forces involved were somewhat small, the yaw moments were significant

NOW AVAILABLE IN PRINT & DIGITAL EDITIONS

SPECIAL SAVINGS WHEN YOU SUBSCRIBE



- NEVER MISS AN ISSUE
- GET IT BEFORE IT HITS THE SHOPS
- KEEP AHEAD OF THE COMPETITION

- READ ON YOUR IPAD, KINDLE OR ANDROID DEVICE
- ACCESS YOUR ARCHIVE AT THE CLICK OF A BUTTON
- ENHANCED DIGITAL CONTENT COMING SOON


Special Subscription Rates: 1 year (12 issues)


Print


UK £44.95 (usually £71.40 - SAVING 37%)
US \$99.95 (usually \$162 - SAVING 38%)
ROW £64.95 (usually £99 - SAVING 35%)

Digital

UK £34.99 (SAVING 51% off the cover price)
US \$49.99 (SAVING 70% off the cover price)
ROW £34.99 (SAVING 65% off the cover price)

 www.chelseamagazines.com/racecar-N407

 +44 (0)1795 419 837 quote N407

 www.chelseamagazines.com/racecar-N407D (for digital)

REF: N407